Structure−Function Studies of Analogues of Parathyroid Hormone (PTH)-1−34 Containing β-Amino Acid Residues in Positions 11−13[†,‡]

E. Peggion,*[,§] S. Mammi,[§] E. Schievano,[§] L. Silvestri,[§] L. Schiebler,[||] A. Bisello,[⊥] M. Rosenblatt,[||] and M. Chorev[||]

University of Padova, Department of Organic Chemistry, Biopolymer Research Center, CNR, Via Marzolo 1, I-35131 Padova, Italy, Bone and Mineral Metabolism Unit, Charles A. Dana Thorndike Laboratories, Department of Medicine, Beth Israel Deaconess Medical Center and Harvard Medical School, 330 Brookline Avenue, Boston, Massachusetts 02215 USA, and Department of Medicine, University of Pittsburgh, Pennsylvania, USA

Received January 8, 2002

ABSTRACT: The 1−34 N-terminal fragments of human parathyroid hormone (PTH) and PTH-related protein (PTHrP) elicit the full spectrum of bone-relevant activities characteristic of the intact hormones. The structural elements believed to be required for receptor binding and biological activity are two helical segments, one N-terminal and one C-terminal, connected by hinges or flexible points located around positions 12 and 19. To test this hypothesis, we synthesized and characterized the following analogues of PTH-(1−34), each containing single or double substitutions with β-amino acid residues around the putative hinge located at position 12: **I.** [Nle^{8,18},β-Ala^{11,12},Nal^{23},Tyr^{34}]bPTH-(1−34)NH$_2$; **II.** [Nle^{8,18},β-Ala^{12,13},Nal^{23},Tyr^{34}]bPTH-(1−34)NH$_2$; **III.** [Nle^{8,18},β-Ala^{11},Nal^{23},Tyr^{34}]bPTH-(1−34)NH$_2$; **IV.** [Nle^{8,18},β-hLeu^{11},Nal^{23},Tyr^{34}]bPTH-(1−34)NH$_2$; **V.** [Nle^{8,18},β-Ala^{12}, Nal^{23},Tyr^{34}]bPTH-(1−34)NH$_2$; **VI.** [Nle^{8,18},β-Ala^{13}, Nal^{23},Tyr^{34}]bPTH-(1−34)NH$_2$ (β-hLeu = β-*homo*-leucine; β-Ala = β-alanine; Nal = L-2-naphthylalanine; Nle = norleucine). Analogues **I** and **III** exhibit very low binding affinity and are devoid of adenylyl cyclase activity. Analogue **II**, despite its very low binding capacity is an agonist. Biological activity and binding capacity are partially restored in analogue **IV**, and completely restored in analogues **V** and **VI**. The conformational properties of the analogues were investigated in aqueous solution containing dodecylphosphocholine (DPC) micelles as a membrane-mimetic environment using CD, 2D-NMR, and molecular dynamics calculations. All peptides fold partially into the α-helical conformation in the presence of DPC micelles, with a maximum helix content in the range of 30−35%. NMR analysis reveals the presence of two helical segments, one N-terminal and one C-terminal, as a common structural motif in all analogues. Incorporation of β-Ala dyads at positions 11,12 and 12,13 in analogues **I** and **II**, respectively, enhances the conformational disorder in this portion of the sequence but also destabilizes the N-terminal helix. This could be one of the possible reasons for the lack of biological activity in these analogues. The partial recovery of binding affinity and biological activity in analogue **IV**, compared to the structurally similar analogue **III**, is clearly the consequence of the reintroduction of Leu side-chain of the native sequence. In the fully active analogues **V** and **VI**, the helix stability at the N-terminus is further increased. Taken together, these results stress the functional importance of the conformational stability of the helical activation domain in PTH-(1−34). Contrary to expectation, insertion of a single β-amino acid residue in positions 11, 12, or 13 in analogues **III**−**VI** does not favor a disordered structure in this portion of the sequence.

Human parathyroid hormone (PTH),[1] an 84-amino acid linear peptide, is a major regulator of calcium homeostasis (*1*). Human parathyroid hormone-related protein (PTHrP), a 139−175 amino acid protein, is a key regulator of cell growth, differentiation, and development of the fetal skeleton, and also plays a major role in the pathogenesis of humoral hypercalcemia of malignancy (*1*−*2*). It has been shown that the N-terminal 1−34 fragments of PTH and PTHrP maintain the same in vitro and in vivo biological activity as the intact

[†] This work is supported, in part, by Grant R01-DK47940 (to M.R.) and by Consiglio Nazionale delle Ricerche (CNR).

[‡] A very preliminary account of this work has been reported in *Peptides. The Wave of the Future*. Proceedings of the Second International and the Seventeenth American Peptide Symposium (Lebl, M., and Houghten, R., Eds.) pp 739−741, American Peptide Society, San Diego, 2001.

* To whom correspondence should be addressed: Dr. E. Peggion, Department of Organic Chemistry, University of Padova, Biopolymer Research Center, Via Marzolo 1, 35131 Padova, Italy. Tel.: 39/049/827-5262. Fax: 39/049/827−5239. E-mail: evaristo.peggion@unipd.it.

[§] Biopolymer Research Center, CNR.

[||] Beth Israel Deaconess Medical Center and Harvard Medical School.

[⊥] University of Pittsburgh.

[1] Abbreviations: Boc, *tert*-butyloxycarbonyl; DCC, *N*,*N*′-dicyclohexylcarbodiimide; D-MEM, Dulbecco's modified Eagle's medium; DPC, dodecylphosphocholine; EDTA, ethylendiaminotetraacetic acid; PTH, parathyroid hormone; PTH1-rc, PTH receptor; PTHrP, PTH-related protein; NMP, *N*-methylpyrrolidone; PBS, phosphate buffer saline; HOBt, *N*-hydroxybenzotriazole; CD, circular dichroism; MD, molecular dynamics; COSY, correlation spectroscopy; NMR, nuclear magnetic resonance; TFA, trifluoroacetic acid; TFE, trifluoroethanol; RP-HPLC, reverse-phase high performance liquid chromatography; IBMX, 3-isobutyl-1-methylxanthine; DQF−COSY, double quantum filtered correlation spectroscopy; TOCSY, total correlation spectroscopy; NOE, nuclear Overhauser enhancement; NOESY, nuclear Overhauser enhancement spectroscopy; DG, distance geometry; SA, simulated annealing.

10.1021/bi0200155 CCC: $22.00
Published on Web 06/01/2002

native sequences, and both interact with PTH1-receptor (PTH1-rc), a cognate class II G protein-coupled receptor, abundant in bone and kidney. Both hPTH-(1−34) and hPTHrP-(1−34) activate at least two signaling pathways through the PTH1-rc: the adenylyl cyclase/PKA and PLC/IP_3/diacylglycerol/intracellular Ca^{2+} transient/PKC pathways (*1*). Signaling for both pathways is initiated through the same receptor, despite the low sequence homology of the two N-terminal fragments. The activation domains, located in the sequence 1−13 of both hormones, share eight identical residues. In the C-terminal region 14−34, where the principal binding domain is located, hPTH-(1−34) and hPTHrP-(1−34) share only three identical residues and differ markedly in the distribution of charges and hydrophobic moieties. On the basis of these observations, the hypothesis was proposed that the two fragments must share the same bioactive conformation at the receptor binding site.

In an effort to determine the structural elements responsible for biological activity, a number of conformational studies, recently reviewed by Wray et al. (*3*), have been carried out by different research groups (*3*−*11*). Although there are some controversial reports from various authors, there is a general agreement on the presence of an essentially random structure in aqueous solution and of a partially ordered structure in water/TFE mixtures or in aqueous solutions containing detergent micelles. The ordered structure consists of two α-helical segments located at the N- and C-termini, connected by a structurally ill-defined region. The presence of these structural elements in solvent systems which are generally considered membrane-mimetic suggests that they are important for bioactivity.

There are discrepant reports regarding the presence of a tertiary structure. Pellegrini et al. (*12*) and Wray et al. (*3*) reported that no unambiguous experimental evidence exists for any significant tertiary structure as suggested in early work (*13*). Weak NOEs indicative of tertiary structure in N-terminal PTH fragments 1−37, 1−34, 3−37, and 4−34 in TFE-free solutions have been reported by Marx et al. (*14*−*15*). However, these authors conclude that, due to the flexibility of the loop region around Gly^{12}, the relative spatial position of the two N- and C-terminal helices is not fixed, and no overall tertiary structure is preferred. In a recent work by the same group (*16*) on PTHrP-(1−34) in near physiological solution, no evidence for interaction between the two helices was obtained by NMR and molecular dynamics calculations. Very recently, the same group (*17*) studied the solution conformations of hPTH-(1−34), hPTH-(1−39), and bPTH-(1−37) in 20% TFE solution. No tertiary structure interactions were observed in this solvent system, and this was attributed to the loss of hydrophobic interactions between Leu^{15} and Trp^{23}. Very recently, Chen et al. (*18*) studied the conformational properties of PTH-(1−31) in aqueous solution containing 25 mM sodium phosphate, 0.2 mM EDTA, and 300 mM NaCl by NMR and structure calculations. The presence of the two N-terminal and C-terminal helices was confirmed, but only very weak interhelical NOEs were found, indicating that there are not very close contacts between the two helices, or that conformational averaging of structures with different relative orientation of the two helices may occur. They concluded that there is a conformation with a bend in the middle of the sequence that is populated sufficiently to give rise to the observed NOE interactions.

In an attempt to gain insight into all structural elements responsible for biological activity of PTH-(1−34) and PTHrP-(1−34), we have carried out conformational studies on a number of active and inactive analogues in membrane-mimetic solvent systems (*8*, *9*, *19*−*21*). The results obtained so far indicate the presence of both the N- and C-terminal helices, and of hinges or flexible regions around positions 12 and 19 in the biologically active analogues. On the basis of these results, the hypothesis was made that hinge or flexibility sites, at distinct positions in the sequence connecting the N- and C-terminal helices, are important structural elements for bioactivity of PTH/PTHrP analogues. These structural motifs could play a functional role in receptor binding and activation events enabling the formation of the bioactive conformation with the correct relative orientation of the two N- and C-terminal helices in the receptor-bound state.

To substantiate this working hypothesis, we designed the following bPTH-(1−34) analogues in which the conformational propensity around the putative hinge site 12 was modified by substitutions with β-Ala or β-hLeu residues:

I. A−V−S−E−I−Q−F−nL−H−N−βA−βA−K−H−L−S−S−nL−E−R−V−E−Nal−L−R−K−K−L−Q−D−V−H−N−Y-NH_2 ([$Nle^{8,18}$, β-$Ala^{11,12}$, Nal^{23},Tyr^{34}]bPTH-(1−34)-NH_2)

II. A−V−S−E−I−Q−F−nL−H−N−L−βA−βA−H−L−S−S−nL−E−R−V−E−Nal−L−R−K−K−L−Q−D−V−H−N−Y-NH_2 ([$Nle^{8,18}$, β-$Ala^{12,13}$,Nal^{23},Tyr^{34}]bPTH-(1−34)-NH_2)

III. A−V−S−E−I−Q−F−nL−H−N−βA−G−K−H−L−S−S−nL−E−R−V−E−Nal−L−R−K−K−L−Q−D−V−H−N−Y-NH_2 ([$Nle^{8,18}$, β-Ala^{11}, Nal^{23},Tyr^{34}]bPTH-(1−34)-NH_2)

IV. A−V−S−E−I−Q−F−nL−H−N−βhL−G−K−H−L−S−S−nL−E−R−V−E−Nal−L−R−K−K−L−Q−D−V−H−N−Y-NH_2 ([$Nle^{8,18}$, β-$hLeu^{11}$, Nal^{23},Tyr^{34}]bPTH-(1−34)-NH_2)

V. A−V−S−E−I−Q−F−nL−H−N−L−βA−K−H−L−S−S−nL−E−R−V−E−Nal−L−R−K−K−L−Q−D−V−H−N−Y-NH_2 ([$Nle^{8,18}$, β-Ala^{12}, Nal^{23},Tyr^{34}]bPTH-(1−34)-NH_2)

VI. A−V−S−E−I−Q−F−nL−H−N−L−G−βA−H−L−S−S−nL−E−R−V−E−Nal−L−R−K−K−L−Q−D−V−H−N−Y-NH_2 ([$Nle^{8,18}$, β-Ala^{13}, Nal^{23}, Tyr^{34}]bPTH-(1−34)-NH_2) (nL = norleucine; βhL = β-hLeu = β-*homo*-leucine; βA = β-Ala = β-alanine; Nal = L-2-naphthylalanine).

The insertion of additional methylene groups in the peptide backbone was expected to increase the conformational flexibility at this position of the sequence.

In the present paper, we report the synthesis, biological evaluation, and conformational characterization by CD, 2D-NMR, and molecular dynamics calculations of these analogues in aqueous solution containing dodecylphosphocholine (DPC) micelles.

EXPERIMENTAL SECTION

Materials. Boc-β-Ala-OH, Boc-Nle-OH, and Boc-2-naphthylalanine (Boc-Nal-OH) were purchased from Bachem Biosciences (King of Prussia, PA). The other Boc-protected amino acids, *N*-hydroxybenzotriazole (HOBt), *N*,*N*′-dicyclohexylcarbodiimide (DCC), and *p*-methylbenzhydrylamine·HCl resin were purchased from Applied Biosystems (Foster

City, CA). B&J brand dichloromethane, *N*-methylpyrrolidone (NMP), and acetonitrile were obtained from Baxter (McGraw Park, IL). Iodogen was purchased from Pierce Chemical Co. (Rockford, IL). [^{125}I]Na was from Amersham Pharmacia Biotech (Arlington Heights, IL). D-MEM, fetal bovine serum, and phosphate buffer saline (PBS) were from Life Technologies, Inc. Tissue culture disposables and plasticware were obtained from Corning (Corning, NY). All other reagents were purchased from Sigma (St. Louis, MO).

Peptide Synthesis. Peptides were synthesized by the solid-phase methodology (*22*) on an Applied Biosystems 430A peptide synthesizer using Boc/HOBt/NMP chemistry and *p*-methylbenzhydrylamine HCl·resin. General protocols for the synthesis, purification, and characterization of peptides are reported elsewhere (*23*−*26*). Specifically, the synthesis was carried out on a 0.5-mmol scale according to the following procedure. The resin-bound side-chain protected Boc[Tyr^{34}]PTH-(25−34) was split into two halves and the stepwise synthesis continued to generate resin-bound side-chain protected Boc[Nle^{18}, Nal^{23}, Tyr^{34}]PTH-(14−34). At this point, the synthesis resumed with aliquots of 0.05 mmol of resin-bound fully protected 21-residue peptide which was carried out to completion. The protocol included double couplings, followed by capping with Ac_2O, for the following positions: Ile^5, Gln^6, Phe^7, Nle^8, Xxx^{11}, Yyy^{12}, Zzz^{13}, His^{14}, Leu^{15}, Glu^{19}, Arg^{20}, Val^{21}, Leu^{22}, Arg^{25}, and Val^{31} (Xxx, Yyy, and Zzz represent either the native residues, Leu, Gly, and Lys, respectively, or the substituting β-Ala or β-hLeu residues). After hydrogen fluoride cleavage, the peptides were purified by preparative reversed-phase high performance liquid chromatography (RP-HPLC). Purity exceeded 97% as determined by analytical RP-HPLC. Structural integrity of the peptides was confirmed by amino acid analysis and electrospray mass spectrometry.

Cell Culture. Human embryonic kidney (HEK293) cells (*27*) stably transfected with recombinant hPTH1-receptor (HEK293/C21 cell line, ∼400 000 receptors/cell ratio) (*28*) were maintained in D-MEM medium supplemented with 10% fetal bovine serum and 2 nM glutamine at 37 °C in a humidified atmosphere of 95% air/5% CO_2. The medium was changed every 3−4 days, and the cells were subcultured every week. Adenylyl cyclase and radioreceptor binding assays were performed on confluent cultures, 1−3 days after a change of medium.

Radioiodinations. PTH-(1−34) was radioiodinated and the crude radioiodinated material was purified as previously described (*29*). Briefly, 67 μg of peptide in 50 μL of phosphate buffer pH 7.4 in a borosilicate tube coated with 10 μg of Iodogen were treated with 2 mCi [^{125}I]Na for 12 min, followed by dilution with 200 μL of 0.1% trifluoroacetic acid (TFA) in water. The pure monoradioiodinated peptide was isolated on an analytical RP-HPLC Vydac Protein C18 column (The Separation Group, Hesperia, CA) employing a linear gradient of 36−42% B in A for 30 min (A = 0.1% TFA in water; B = 0.1% TFA in acetonitrile) at a flow rate of 1 mL/min, and monitored at 220 nm.

Competition Binding Assay. Cells were plated in 24-well tissue culture dishes (Corning Glass Works, Corning, NY) and grown to subconfluency. The cells were then incubated for 2 h at room temperature in fresh PBS supplemented medium (0.25 mL) containing 100 000 cpm (∼0.1 nM) radioiodinated ligand (^{125}I-PTH-(1−34)) in the absence or presence of increasing concentrations of unlabeled competing bPTH-(1−34) or analogues **I**−**VI**. Following incubation, cells were washed twice with PBS and lysed with 0.1 M NaOH. Radioactivity in the lysate was measured in a γ-counter (TmAnalytic GammaTrac 1193).

Adenylyl Cyclase Activation Assay. Stimulation of adenylyl cyclase activity by the bPTH-(1−34) analogues was assayed in stably transfected HEK293/C21 as described before (*25*). Briefly, cells were grown to confluence in 24-well culture dishes. They were then incubated with 0.5 μCi [^{3}H]adenine in fresh PBS-supplemented medium at 37 °C for 2 h and further treated with 1 mM 3-isobutyl-1-methylxantine (IBMX) in fresh medium for 15 min at 37 °C. This treatment was followed by 5 min incubation with the corresponding analogue. The reaction was terminated by adding 1.2 M trichloroacetic acid and neutralizing with 4 N KOH. cAMP was isolated by the two-column chromatographic method (*30*). Radioactivity was measured in a scintillation counter (Beckman LS6000IC liquid scintillation counter, Downers Grove, IL).

CD Experiments. CD measurements were carried out on a JASCO J-715 spectropolarimeter interfaced with a PC. The CD spectra were acquired and processed using the J-700 program for Windows. All experiments were carried out at room temperature using HELLMA quartz cells with Suprasil windows and optical path-length of 0.1 cm. All spectra were recorded using a bandwidth of 2 nm and a time constant of 2−8 s at a scan speed of 20 or 50 nm/min. The signal-to-noise ratio was improved by accumulating at least six scans. The helix content of each peptide was estimated according to the method of Greenfield and Fasman (*31*).

The concentrations of the peptide solutions were determined by UV absorption measurements with a Perkin-Elmer Lambda 5 spectrophotometer interfaced with a Perkin-Elmer Lambda computer. The molar absorbivities values at 276 nm of tyrosine and 2-naphthylalanine are 1400 and 4330 L M^{-1} cm^{-1}, respectively. The ϵ value of the naphthyl chromophore in the micellar solution was experimentally determined using Boc-2-naphthylalanyl-amide.

NMR Experiments. NMR experiments were performed on a BRUKER AVANCE DMX 600 spectrometer. The measurements were carried out at 313 K on 1.5 mM peptide solutions in H_2O/D_2O 9:1 containing 0.22−0.36 M deuterated dodecylphosphocholine (DPC-d_{38}). The CD spectra of these solutions were identical to those of the more dilute solutions used for CD measurements. Tetramethylsilane was used as internal standard. The water signal was suppressed using the WATERGATE pulse sequence (*32*). For each peptide, the complete assignment of the spin systems was achieved from DQF−COSY (*33*) and CLEAN-TOCSY (*34*−*35*) spectra, while NOESY experiments (*36*) were used for sequential assignment. All spectra were acquired by collecting 300−600 experiments, each one consisting of 40−68 scans in 2048 data points in t_2. NOE build-up curves were generated for different dipolar correlations and found to be linear up to 70 ms mixing time (data not shown). This value was therefore used in all NOESY experiments to avoid the problem of spin diffusion. To resolve ambiguous and overlapped NOE peaks in the normal NOESY experiments arising from low F1 resolution (6.4 Hz per point), semi-soft NOESY (*37*) experiments with digital resolution of 0.7 Hz per point in F1 were acquired. A G4 shaped pulse, centered

Table 1: Biological Activity of PTH Analogues Substituted at Positions 11, 12, and 13 (HEK-293/C-21 cells)

analogue	EC_{50} (nM)[a,b]	IC_{50} (nM)[c]
[Nle^{8,18},Nal^{23},Tyr^{34}]-bPTH−(1−34)NH_2	0.85 ± 0.1	12 ± 0.5
I. [Nle^{8,18},β-Ala^{11,12},Nal^{23},Tyr^{34}]-bPTH-(1−34)-NH_2	>1000	>1000
II. [Nle^{8,18},β-Ala^{12,13},Nal^{23},Tyr^{34}] bPTH-(1−34)-NH_2	8.5 ± 1.5	>1000
III. [Nle^{8,18},β-Ala^{11},Nal^{23},Tyr^{34}] bPTH-(1−34)-NH_2	>500	>1000
IV. [Nle^{8,18},h-Leu^{11}, Nal^{23},Tyr^{34}] bPTH-(1−34)-NH_2	50 ± 1.5	80
V. [Nle^{8,18},β-Ala^{12}, Nal^{23},Tyr^{34}] bPTH-(1−34)-NH_2	0.7 ± 0.07	150 ± 13
VI. [Nle^{8,18},β-Ala^{13}, Nal^{23},Tyr^{34}] bPTH-(1−34)-NH_2	0.3 ± 0.1	23 ± 1

[a] Stimulation of adenylyl cyclase activity, 5 min exposure to ligand. [b] E_{max} (fold above basal): 50 ± 7 (parent compound); 49 ± 2 (**II**); 56 ± 2 (**V**); 55 ± 5 (**VI**). [c] Competition of ^{125}I-PTH-(1−34) binding.

in the Hα region, was used to replace the first 90° hard pulse. To verify the compatibility of the distance values obtained by semi-soft NOESY with the restraints extracted from standard NOESY, the effect of the offset position in the F1 dimension on the volumes of integrated cross-peaks was examined. The distances extracted from several semi-soft NOESY experiments were identical to those obtained from normal NOESY, within an accuracy of 5%, attesting a negligible effect of the offset.

Interproton distances were obtained by integration of the NOESY cross-peaks using the AURELIA software package (*38*). The calibration was based on the cross-peaks of the geminal protons of Tyr^{34} or Ser^{3} set to a distance of 1.78 Å. Addition and subtraction of 10% of the calculated distances yielded upper and lower bounds. An upper limit of 4 Å was arbitrarily set for overlapped cross-peaks.

Structure Calculations. Distance geometry (DG) and molecular dynamics (MD) calculations were carried out using the simulated annealing (SA) protocol of the X-PLOR 3.0 program (*39*). For distances involving equivalent or nonstereo-assigned protons, r^{-6} averaging was used. The general procedure of the MD calculations involved a minimization step of 200 cycles, followed by an SA and a refinement stage. The SA consisted of two phases: (i) 30 ps of dynamics at 1500 K (10000 cycles, in 3 fs steps); (ii) 30 ps of cooling from 1500 to 100 K in 50 K decrements (15000 cycles, in 2 fs steps). The SA procedure, in which the weights of NOE and nonbonded terms were gradually increased, was followed by 200 cycles of energy minimization. In the refinement stage, the system was cooled from 1000 to 100 K in 50 K decrements (10000 cycles, in 1 fs steps). Finally, the calculation was completed with 200 cycles of energy minimization using a NOE force constant of 50 kcal/mol.

RESULTS

Binding Affinity and Ligand-Stimulated cAMP Accumulation. The results of the biological characterization of the analogues, including receptor binding affinity and efficacy in stimulating accumulation of cAMP, are reported in Table 1. Analogues **II**, **IV**−**VI** were full agonists with E_{max} of about 50-fold above basal. Insertion of β-Ala dyads into the biologically active [Nle^{8,18},Nal^{23},Tyr^{34}]bPTH-(1−34)-NH_2 parent compound generated the weakly binding analogues **I** and **II**. Analogue **II**, despite its low binding affinity is an agonist (about 10 times less potent than the parent compound). The monosubstituted analogue **III** containing a β-Ala residue at position 11 is devoid of binding affinity and inactive. Interestingly enough, reintroduction of the Leu^{11} side-chain by insertion of β-*homo*-Leu leads to a partial recovery of biological activity and binding capacity in analogue **IV**, with EC_{50} and IC_{50} higher by 60- and 6-fold than the respective values for the parent compound. Analogue **V** is about equally potent in the adenylyl cyclase stimulatory activity and about 12-fold weaker in binding affinity as compared to the parent compound. Finally, analogue **VI**, compared to the parent peptide, is about 3-fold more potent and has comparable binding affinity.

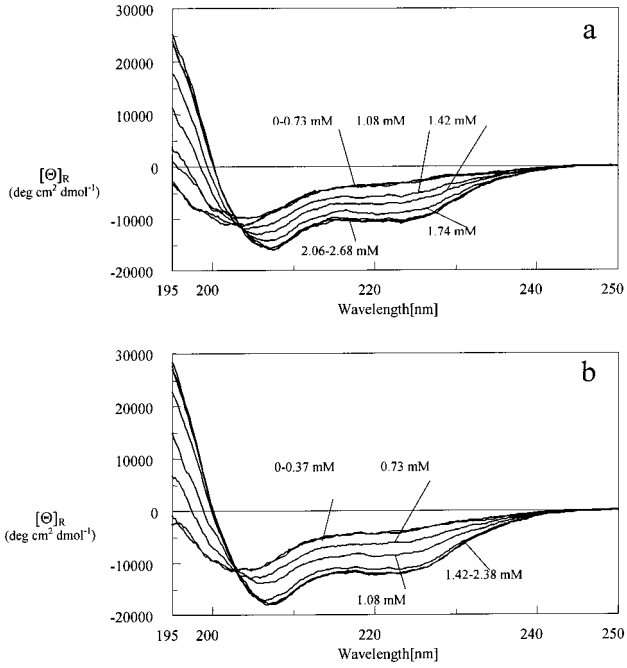

FIGURE 1: CD spectra of analogue **III** (a), 4.91×10^{-5} M; analogue **V** (b), 5.22×10^{-5} M, in water at increasing concentrations of DPC (indicated in the spectra).

CD Results. The different sequence modifications introduced in the six analogues do not have major effects on their chiroptical properties. As an example, the CD spectra of analogues **III** and **V** recorded in aqueous solution in the presence of increasing amounts of DPC are shown in Figure 1. The other analogues exhibit practically the same behavior (Figures 1 and 2 of Supporting Information). In all cases, the set of spectra recorded at increasing detergent concentrations fit the same isodichroic point around 203 nm, typical of the two component coil−helix equilibrium system. In the absence of detergent, the CD spectra of the six analogues indicate the presence of a predominantly random conformation with a small amount of ordered structure, as revealed by the shoulder around 222 nm. Increase of the detergent concentration above the critical micellar concentration results in the development of the typical CD pattern of the right-handed α-helix with the classic two negative maxima at 208 and 222 nm. This indicates a shift of the equilibrium in the conformer population toward the ordered structure. At saturation conditions, the maximum helix content is in the range of 30−35% for all analogues. As reported previously (*20*), these findings confirm that in the aqueous medium the

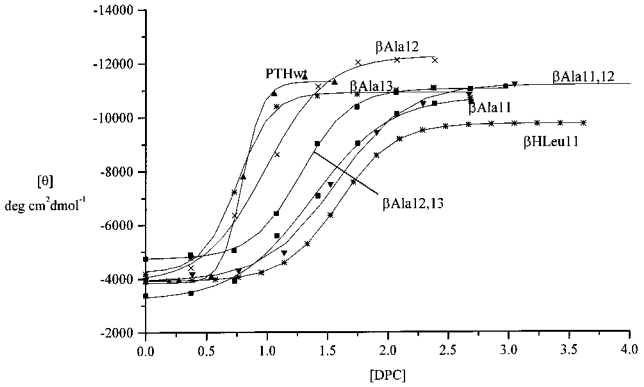

FIGURE 2: Molar ellipticity at 222 nm of analogues **I**−**VI** as a function of DPC concentration. The results obtained with unmodified PTH-(1−34) (PTHwt) are shown for comparison.

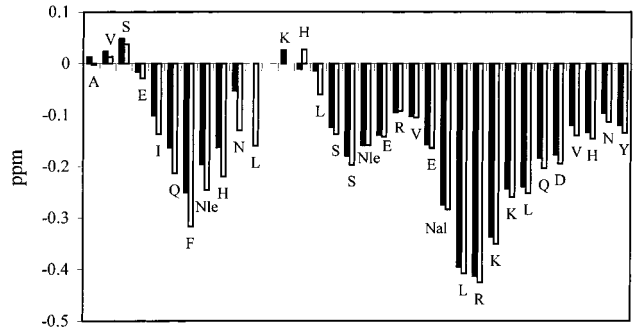

FIGURE 3: Chemical shift differences (ppm) of the αH protons relative to the random coil values of analogue **I** (filled bars) and **II** (empty bars). The values relative to the *β*-Ala residues are missing because the reference random coil chemical shift for this residue is not available.

presence of micelles is required to reach the maximum helix content. The profiles of molar ellipticity values at 222 nm as a function of DPC concentration are shown in Figure 2. In the same figure, the results obtained with native PTH-(1−34) are reported for comparison. All curves are S-shaped, indicative of a cooperative conformational change. The fully active analogues **V** and **VI**, which contain a single *β*-Ala residue at positions 12 and 13, respectively, show profiles very similar to that of the native sequence. Conversely, all analogues containing substitutions at position 11 (**I**, **III**, and **IV**) exhibit consistent shifts of the half-transition points to higher DPC concentrations, indicating a lower tendency to fold into the α-helical conformation. The profile of the disubstituted analogue **II**, which contains the dyad *β*-Ala^{12}−*β*-Ala^{13}, is between that of the native sequence and those of analogues **I**, **III**, and **IV**. Thus, the conformational change occurs at lower DPC concentration upon shifting the *β*-amino acid residue from position 11 toward the middle of the sequence. This is an indication that the enhancement of the conformational preference for the α-helical conformation consequent to the displacement of *β*-amino acid residues far from the N-terminus mainly involves the N-terminal helical segment.

NMR Results. Examples of the fingerprint regions of NOESY spectra of the analogues are shown in Figures 1 and 2 of the Supporting Information. The summary of proton resonance assignments is reported in Tables 1−6 of the Supporting Information.

(a) Secondary Shifts of αH Protons. The chemical shift differences of the αCH protons of analogues **I** and **II** with

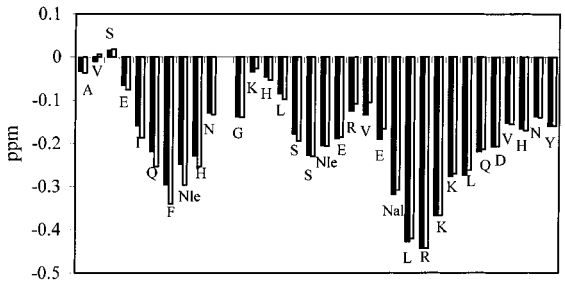

FIGURE 4: Chemical shift differences (ppm) of the αH protons relative to the random coil values of analogue **III** (filled bars) and **IV** (empty bars).

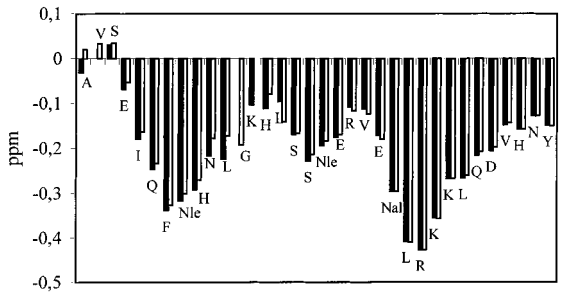

FIGURE 5: Chemical shift differences (ppm) of the αH protons relative to the random coil values of **V (**filled bars) and **VI** (empty bars).

respect to the corresponding random coil values are shown in Figure 3. The random coil αCH chemical shifts of Leu and Phe were used as reference values for Nle and Nal, respectively. Negative values of the order of 0.1 ppm or higher, consistent with the presence of the α-helical structure (*40*), span the N-terminal sequence from Ile^5 to His^9 in analogue **I** and from Ile^5 to Leu^{11} in analogue **II**. The helical structure in these two analogues is clearly interrupted around the *β*-Ala dyads with slightly positive values for Lys^{13} and His^{14}, respectively. Then, the helical structure is resumed starting from Ser^{16}, spanning the entire C-terminal sequence. There is a minimum around Arg^{20}, which might indicate the presence of a bend or kink in the helix. The presence of the bulky aromatic *β*-2-naphthylalanine residue at position 23 could affect the chemical shift of protons in its neighborhood due to the anisotropic effect of the ring current. The values reported in Figure 3 were obtained by averaging the secondary shifts with those of neighboring residues. Consequently, the anisotropic effect should be minimized, and the minimum around position 20 should be real. The difference between the secondary chemical shifts of the αCH protons of the two analogues, shown in Figure 3, yields more negative values in the N-terminal segment of analogue **II**, indicating a slightly higher stability of the helical structure.

The chemical shift differences of the αCH protons of the monosubstituted analogues **III** and **IV** with respect to the corresponding random coil values are shown in Figure 4. The profiles of the two analogues are very similar and identify two stretches of helix at the N- and C-terminal regions of the peptide sequence. The slightly more negative values observed in the segment Glu^4−His^9 of analogue **IV** suggest that the presence of the isobutyl side-chain of hLeu also contributes to the stability of the N-terminal helix. Noticeably, for both analogues, negative values higher than 0.1 are found also for the Gly^{12} residue, which indicates that the N-terminal helix extends until position 12, comprising

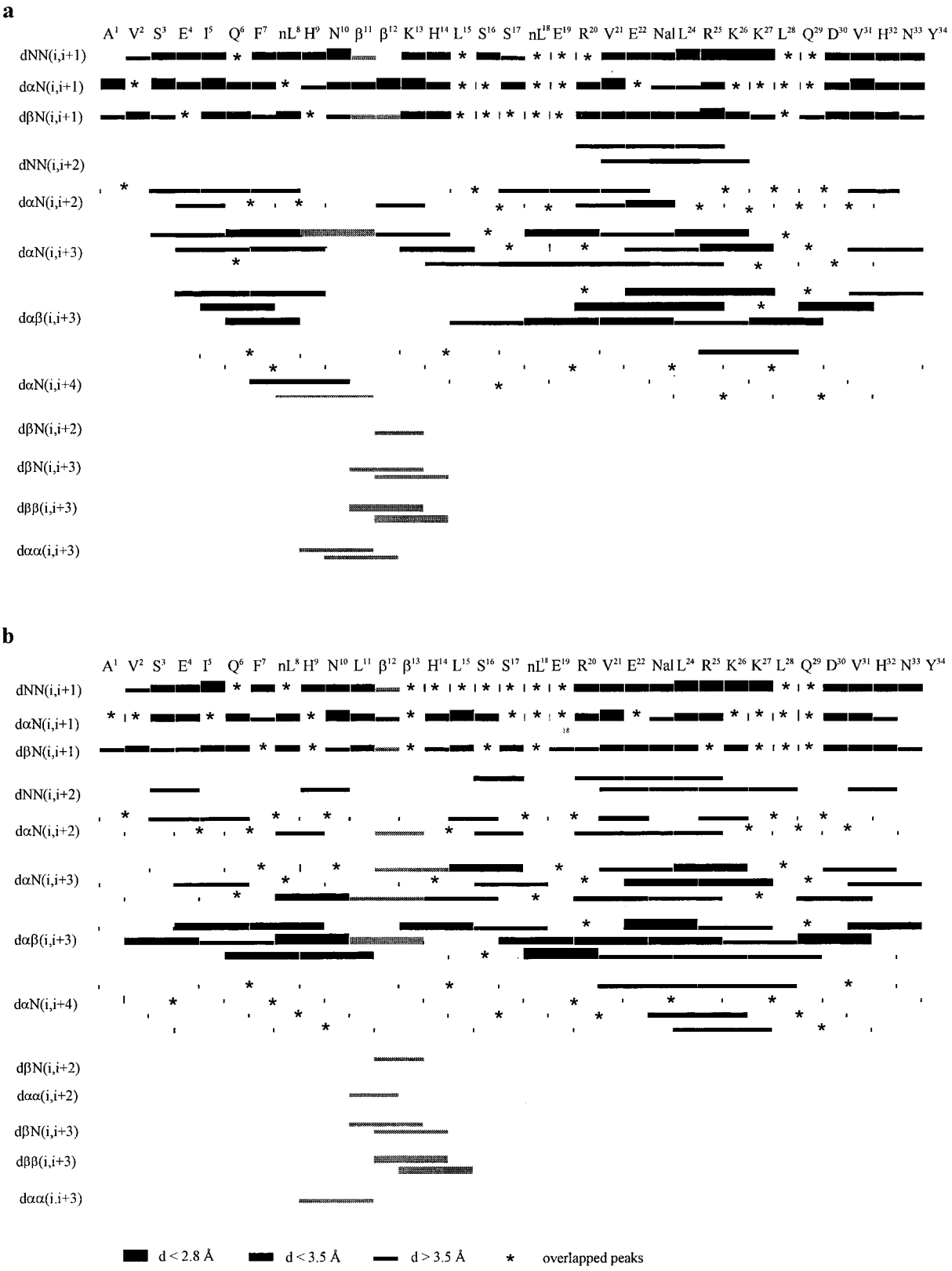

FIGURE 6: Summary of NOESY connectivities of analogue **I** (a) and **II** (b) in water containing DPC micelles. Peaks are grouped in three classes, based upon their integrated volumes. Shaded bars indicate nonstandard interactions involving β-amino acid residues.

the β-amino acid residue. The helical structure is clearly interrupted around positions 13−14, with small, negative chemical shift differences. A minimum is again present around position 20 of both analogues, interpreted as indicative of a bend or kink of the helix.

The chemical shift differences of the αCH protons of the monosubstituted analogues **V** and **VI** with respect to the corresponding random coil values are shown in Figure 5. Also in this case, the profiles are almost overlapping and slightly but distinctly different from those of the other two

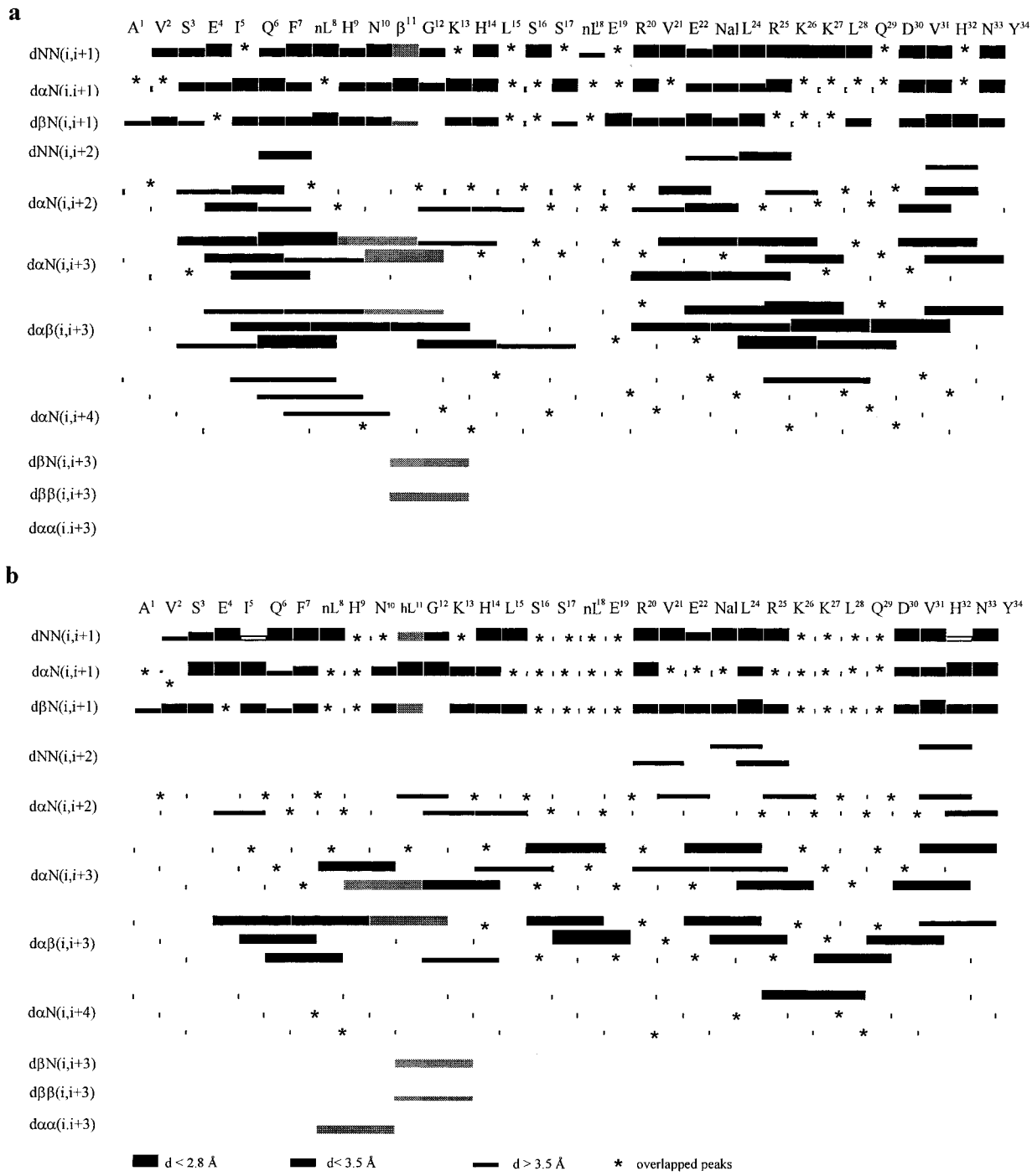

FIGURE 7: Summary of NOESY connectivities of analogue **III** (a) and **IV** (b) in water containing DPC micelles. Peaks are grouped in three classes, based upon their integrated volumes. Shaded bars indicate nonstandard interactions involving β-amino acid residues.

analogues monosubstituted in position 11. In fact, negative values of the chemical shift differences consistent with the presence of the helical structure are spanning the sequence from Ile[5] to Tyr[34]. In analogue **VI**, Gly[12] is included in the helical segment. The minima around positions 13 (much less deep than in analogues **III** and **IV**) and 20 are compatible with the presence of kinks or bends of the helix. The negative values of the chemical shift differences observed in the N-terminal sequence are slightly larger than in analogues **III** and **IV** (Figure 5), indicating a higher stability of the N-terminal helix. Taken together, the results of chemical shift differences presented above support the conclusion based on CD results that in all mono- and disubstituted analogues the shift of β-amino acid residues from position 11 or 12 toward the middle of the sequence enhances the stability of the N-terminal helix. Interestingly enough, the chemical shift results indicate that in all monosubstituted analogues, the Gly[12] residue (not present in analogue **V**) and the β-amino acid residues are included in the N-terminal helical segment.

(b) NOESY Results. The patterns of sequential and medium range NOESY connectivities of all analogues relevant for the assessment of secondary structure are shown in Figures 6−8. No long-range connectivities were observed in any of the analogues reported in the present study. In analogues **I** and **II**, a number of αH(i)−βH(i+3) interactions, indicative of the α-helical conformation, span the N-terminal and

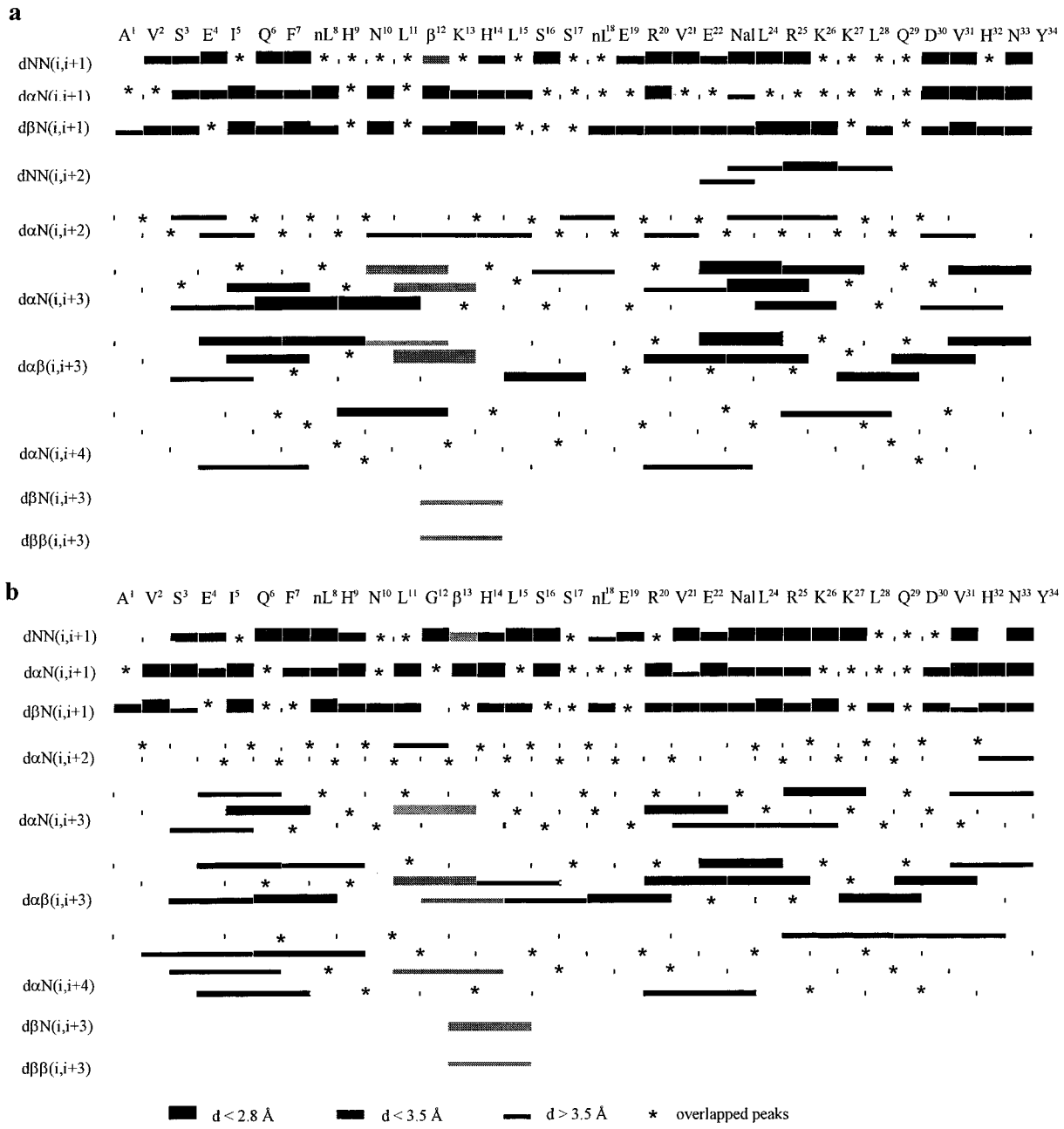

FIGURE 8: Summary of NOESY connectivities of analogues **V** (a) and **VI** (b) in DPC micelles. Peaks are grouped in three classes, based upon their integrated volumes. Shaded bars indicate nonstandard interactions involving β-amino acid residues.

C-terminal sequences, along with sequential NH(i)−NH(i+1) and medium range αH(i)−HN(i+3) connectivities. However, in the N-terminal region a few i, i+3 cross-peaks are missing. In the C-terminal region of the two analogues, particularly in analogue **II**, starting from Ser[17]−Nle[18], there is a higher number of i, i+3 NOE connectivities than in the N-terminal region and, in the case of analogue **II**, also four αH−HN (i, i+4) connectivities. The higher concentration of helical NOEs indicates a higher stability of the helical structure in the C-terminal domains compared to the N-terminal ones. Consistent with the results of chemical shift differences reported above, in the segment Asn[10]−His[14] comprising the β-Ala dyads, there is a lack of helical NOEs, more pronounced for analogue **I**, indicating an interruption of the helical segment in this part of the sequence.

In all monosubstituted analogues **III**−**VI**, the NOE pattern confirms the presence of two helical segments at the N- and C-terminal portions the molecules (Figures 7−8). Again, a higher concentration of i, i+3 NOEs is found in the C-terminal sequence Arg[20]−Asn[33], indicating a higher stability of the helical structure in this region. As compared to the doubly substituted analogues, a slightly higher number of i, i+2 connectivities, usually indicative of 3_{10}-helices or β-turn-like structures, are present in the segment Asn[10]−His[14] comprising the substitution positions 11, 12, and 13. Consistent with the chemical shift results, these findings indicate that the β-amino acid residues are contained within the N-terminal helical segment.

Structure Calculations. (a) Analogues I−*II.* Distance restraints were derived from integration of the NOESY spectra and yielded 307 and 372 interproton distances for analogue **I** and **II**, respectively (Table 2). Using the SA protocol of the X-PLOR program previously described, 150 structures were generated, of which 77 (**I**) and 58 (**II**)

Table 2: NOE Restraints, Deviations from Idealized Geometry, and Mean Energies of the NMR-Based Structures

analogue	**I**	**II**	**III**	**IV**	**V**	**VI**
			No. of NOEs			
total	307	372	338	331	323	257
intraresidue	105	128	135	120	134	112
sequential	113	123	110	108	98	93
i/i + *n*, *n* = 2, 3, 4	89	121	93	103	91	52
			Mean rmsd from Ideality for Accepted Structures			
bonds (Å)	$(4.2 \pm 0.2) \times 10^{-3}$	$(5.2 \pm 0.2) \times 10^{-3}$	$(7.1 \pm 0.2) \times 10^{-3}$	$(5.4 \pm 0.2) \times 10^{-3}$	$(7.81 \pm 0.19) \times 10^{-3}$	$(5.8 \pm 0.3) \times 10^{-3}$
angles (deg)	0.61 ± 0.02	0.68 ± 0.03	0.71 ± 0.02	0.575 ± 0.013	0.72 ± 0.02	0.579 ± 0.018
improper (deg)	0.49 ± 0.09	0.57 ± 0.05	0.67 ± 0.05	0.31 ± 0.04	0.82 ± 0.07	0.38 ± 0.05
NOE (Å)	$(8.2 \pm 0.4) \times 10^{-2}$	$(9.9 \pm 0.3) \times 10^{-2}$	$(11.9 \pm 0.3) \times 10^{-2}$	$(8.3 \pm 0.3) \times 10^{-2}$	$(11.8 \pm 0.2) \times 10^{-2}$	$(11.1 \pm 0.5) \times 10^{-2}$
			Mean Energies (kcal/mol) of Accepted Structures			
$E_{overall}$	187 ± 12	293 ± 17	374 ± 17	187 ± 8	373 ± 12	242 ± 19
E_{bond}	10.8 ± 0.9	15.6 ± 1.4	29.5 ± 1.6	17.2 ± 1.0	36.4 ± 1.8	19 ± 2
E_{angle}	61 ± 4	75 ± 6	81 ± 5	54 ± 2	86 ± 4	53 ± 3
E_{NOE}	103 ± 10	184 ± 12	241 ± 13	111 ± 7	223 ± 8	159 ± 14

Table 3: Average Values of Torsion Angles ϕ, ψ, μ, and the Relative Standard Deviations Resulting from the Lowest 20 Energy Structures Calculated for Analogues **I** and **II**

	analogue **I**				analogue **II**		
residue	ϕ	ψ	μ	residue	ϕ	ψ	μ
Ala[1]		72 ± 52		Ala[1]		84 ± 30	
Val[2]	-179 ± 26	25 ± 50		Val[2]	19 ± 60	-40 ± 28	
Ser[3]	-102 ± 46	70 ± 87		Ser[3]	-28 ± 34	6 ± 51	
Glu[4]	33 ± 63	-34 ± 7		Glu[4]	-17 ± 49	-9 ± 30	
Ile[5]	-80 ± 28	-23 ± 7		Ile[5]	-92 ± 22	-42 ± 17	
Gln[6]	-74 ± 11	-33 ± 3		Gln[6]	-76 ± 11	-35 ± 12	
Phe[7]	-73 ± 4	-31 ± 3		Phe[7]	-62 ± 10	-41 ± 4	
Nle[8]	-76 ± 3	-33 ± 6		Nle[8]	-62 ± 4	-41 ± 2	
His[9]	-62 ± 7	-52 ± 10		His[9]	-60 ± 3	-47 ± 2	
Asn[10]	-75 ± 10	-16 ± 10		Asn[10]	-68 ± 6	-12 ± 7	
β-Ala[11]	-131 ± 22	-131 ± 48	79 ± 55	Leu[11]	-116 ± 17	4 ± 50	
β-Ala[12]	-150 ± 74	-139 ± 87	85 ± 60	β-Ala[12]	-167 ± 61	36 ± 93	69 ± 21
Lys[13]	-11 ± 75	-37 ± 19		β-Ala[13]	120 ± 77	-65 ± 10	83 ± 13
His[14]	-94 ± 10	11 ± 8		His[14]	-125 ± 6	-14 ± 6	
Leu[15]	-137 ± 26	-3 ± 7		Leu[15]	-127 ± 8	-22 ± 11	
Ser[16]	-50 ± 75	-22 ± 67		Ser[16]	-69 ± 10	-22 ± 30	
Ser[17]	-51 ± 70	36 ± 20		Ser[17]	-77 ± 31	-23 ± 9	
Nle[18]	-82 ± 28	-13 ± 19		Nle[18]	-93 ± 13	-47 ± 12	
Glu[19]	-85 ± 22	-24 ± 12		Glu[19]	-52 ± 14	-41 ± 11	
Arg[20]	-89 ± 13	-10 ± 10		Arg[20]	-70 ± 11	-29 ± 3	
Val[21]	-78 ± 20	-42 ± 49		Val[21]	-69 ± 5	-33 ± 13	
Glu[22]	-52 ± 62	-40 ± 7		Glu[22]	-79 ± 11	-40 ± 3	
Nal[23]	-67 ± 5	-27 ± 5		Nal[23]	-67 ± 4	-26 ± 5	
Leu[24]	-79 ± 5	-40 ± 4		Leu[24]	-80 ± 4	-36 ± 3	
Arg[25]	-66 ± 10	-47 ± 11		Arg[25]	-60 ± 6	-42 ± 6	
Lys[26]	-53 ± 10	-40 ± 6		Lys[26]	-71 ± 7	-35 ± 6	
Lys[27]	-70 ± 7	-36 ± 4		Lys[27]	-79 ± 8	-21 ± 10	
Leu[28]	-74 ± 5	-27 ± 9		Leu[28]	-83 ± 10	-31 ± 11	
Gln[29]	-77 ± 12	-29 ± 7		Gln[29]	-95 ± 14	-11 ± 9	
Asp[30]	-84 ± 6	-31 ± 4		Asp[30]	-83 ± 9	-33 ± 8	
Val[31]	-75 ± 8	-13 ± 9		Val[31]	-68 ± 10	-36 ± 5	
His[32]	-58 ± 9	-26 ± 11		His[32]	-75 ± 5	-40 ± 9	
Asn[33]	-92 ± 14	8 ± 9		Asn[33]	-80 ± 8	5 ± 11	
Tyr[34]	-131 ± 12			Tyr[34]	-117 ± 25		

fulfilled the experimentally determined interproton distances with violations lower than 0.5 Å (Table 2). The average ϕ and ψ backbone dihedral angles of two ensembles of the 20 lowest energy structures, with relative standard deviations, are reported in Table 3. Spread of dihedral angles is observed in the 1−6 and 11−22 sequences of analogue **I**, and 1−6 and 11−21 sequences of analogue **II**. There is also a large spread of the three backbone dihedral angles ϕ, ψ, and μ of the β-Ala dyads, indicating that there is no convergence to a well-defined structure. The superimposition of the ensemble of lowest energy structures of analogues **I** and **II** is shown in Figure 9. Only portions of the sequences are shown for clarity. The convergence of the C-terminal and N-terminal sequences to the α-helical structure is clearly evident.

(b) Analogues III−VI. Integration of the NOESY spectra yielded 338, 331, 312, and 256 interproton distances for analogue **III**, **IV**, **V**, and **VI**, respectively. Following the same protocol described above, 150 structures were generated, of which 47 (**III**), 45 (**IV**), 57 (**V**), and 40 (**VI**) had violations of the experimentally derived interproton distances lower than 0.5 Å (Table 2). The average backbone dihedral angles of the 20 lowest energy structures of each analogue, with the relative standard deviations, are reported

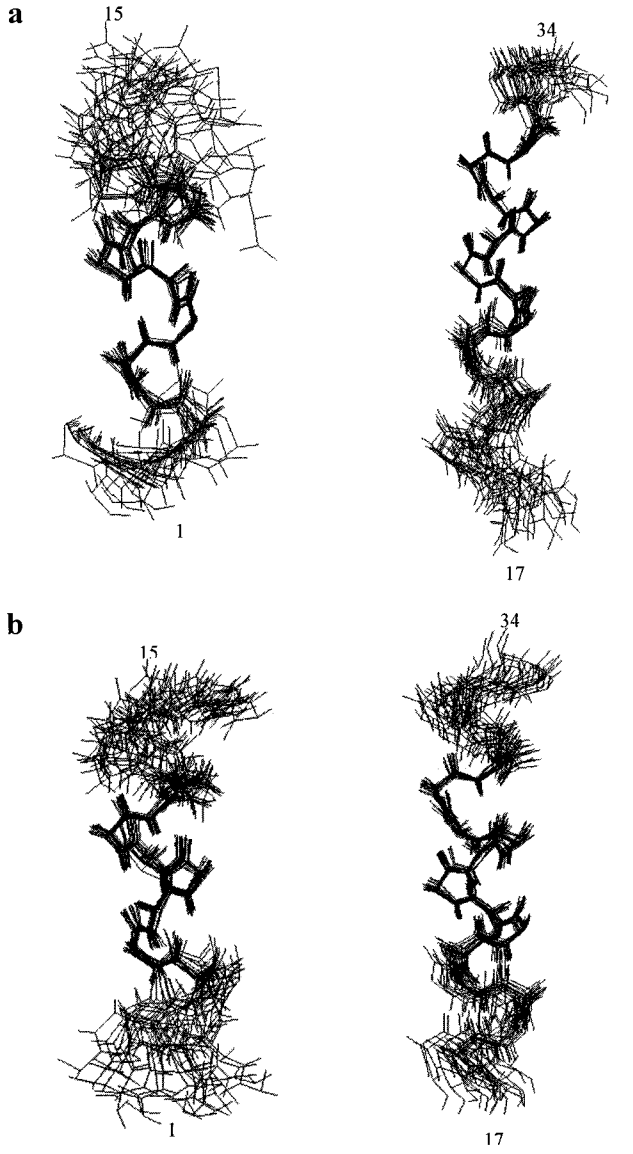

FIGURE 9: Superimposition of the ensemble of the 20 lowest energy calculated structures of analogue **I** (a) and **II** (b). Heavy backbone atoms of the 5−11 and 24−31 sequences were used in the superimposition, respectively. Only portions of the sequences are shown for clarity.

in Tables 4−5. A spread distribution of backbone dihedral angles of the ensembles of calculated structures is observed at the N-terminal segments 1−5 and in the central segments 15−19 of all analogues. Conversely, in all analogues the structural ensembles converge to a relatively well-defined set of dihedral angles in the sequences 6−12, 6−12, 6−13, and 6−14 of analogues **III**, **IV**, **V**, and **VI**, respectively, and in the C-terminal portion of sequences starting from position 20 of all four analogues. Interestingly enough, in all low energy calculated structures of analogues **III** to **VI**, a small spread of the values of dihedral angles is observed for the β-amino acid residues, indicating convergence to a well-defined structure. From the superimposition of the backbone heavy atoms of the N- and C-terminal sequences of the ensembles of lowest energy calculated structures, the convergence to two α-helical segments is clearly evident (data not shown). An interesting result is obtained from the superimposition of the 20 lowest energy structures by overlapping the backbone heavy atoms of the sequence 10−14 (Figure 10). The convergence of all structures to a well-defined conformation in this segment is clearly evident. Most important, the overlap of the backbone atoms of the sequences 10−14 leads to convergence in the N-terminal α-helical segments.

DISCUSSION AND CONCLUSIONS

The results presented in this work show that all PTH analogues, either biologically active or inactive, exhibit the common structural motif of two helical segments, one at the N- and one at C-terminus. Our findings confirm that the presence of these structural elements is a necessary, but not sufficient, condition for the expression of biological activity of PTH-(1−34). For all the analogues studied in this work, the results of NMR analysis and MD calculations are consistent with a higher stability of the C-terminal helix with respect to the N-terminal one. The NOE data indicate that in all peptides approximately 22 amino acid residues, i.e., ∼70% of the entire sequence, are comprised in helical segments. This helical content is higher than that detected by the CD analysis and indicates that, in the membrane-mimetic micellar system, the overall conformation is rather flexible and that for each analogue there is an ensemble of conformers in dynamic equilibrium. In such equilibrium systems, composed of conformers with different helix content in fast exchange on the NMR time scale, the NOE data represent the time-averaged situation and overemphasize the ordered structure content of the whole sequence. Since in all analogues the C-terminal helix is more stable than the N-terminal one, most of the structural differences among the members of the conformer ensembles are very likely located in the middle and N-terminal regions of the sequences.

In all analogues studied in the present work, the substitutions with β-amino acid residues around position 12 have significant structural consequences. According to our working hypothesis, based upon previous work, hinges or flexible regions around positions 12 and 19 are important structural features of the bioactive conformation. Insertion of the β-Ala−β-Ala dyad in analogues **I** and **II** increases the flexibility in the central segment. However, this substitution also reduces the stability of the N-terminal helix with respect to that observed in the native sequence in the same solvent system (*12*). The lower stability of the N-terminal helix could be one of the factors responsible for the loss of biological activity and binding affinity of these two analogues. The partial recovery of agonistic activity in analogue **II** could be in part attributed to the slightly higher stability of the N-terminal helix as compared to that of analogue **I**. However, an additional factor affecting the different biological activity of these two analogues is suggested by the results obtained with the monosubstituted analogues **III**−**IV**, which are structurally very similar. The fact that analogue **III** containing β-Ala^{11} is inactive, while partial activity is restored in analogue **IV** containing β-hLeu^{11}, underlines the importance of the side-chain of Leu^{11} for bioactivity. This implies that the lack of the important aliphatic isobutyl side-chain in position 11 contributes to the elimination of biological activity in analogue **I**, containing the β-Ala^{11,12} dyad. This conclusion is in line with previous studies on the biological properties of PTH and PTHrP-derived 7−34 peptides with swapped residues in position 11 (*41*). This modification removed residual agonist properties from the PTHrP/PTH

Table 4: Average Values of Torsion Angles ϕ, ψ, μ, and the Relative Standard Deviations Resulting from the Lowest 20 Energy Structures Calculated for Analogues **III** and **IV**

	analogue **III**				analogue **IV**		
residue	ϕ	ψ	μ	residue	ϕ	ψ	μ
Ala[1]		37 ± 84		Ala[1]		101 ± 62	
Val[2]	5 ± 8	-59 ± 19		Val[2]	51 ± 42	-50 ± 4	
Ser[3]	-163 ± 35	110 ± 77		Ser[3]	-151 ± 78	172 ± 83	
Glu[4]	-53 ± 52	-2 ± 26		Glu[4]	-66 ± 88	44 ± 46	
Ile[5]	-112 ± 26	-20 ± 9		Ile[5]	-76 ± 33	-32 ± 3	
Gln[6]	-72 ± 6	-24 ± 3		Gln[6]	-42 ± 2	-34 ± 7	
Phe[7]	-80 ± 3	-16 ± 1		Phe[7]	-65 ± 10	-28 ± 3	
Nle[8]	-93 ± 2	-36 ± 2		Nle[8]	-79 ± 4	-27 ± 5	
His[9]	-66 ± 4	-40 ± 2		His[9]	-86 ± 5	-31 ± 3	
Asn[10]	-90 ± 4	-17 ± 9		Asn[10]	-86 ± 2	-19 ± 1	
β-Ala[11]	-116 ± 10	-90 ± 10	67 ± 3	hLeu[11]	-140 ± 2	-127 ± 1	113 ± 1
Gly[12]	-45 ± 6	-35 ± 12		Gly[12]	-63 ± 3	-27 ± 4	
Lys[13]	-80 ± 18	-8 ± 9		Lys[13]	-52 ± 5	-22 ± 8	
His[14]	-123 ± 12	15 ± 7		His[14]	-95 ± 7	-9 ± 7	
Leu[15]	-78 ± 21	-8 ± 30		Leu[15]	-85 ± 14	-20 ± 9	
Ser[16]	-86 ± 53	5 ± 9		Ser[16]	-77 ± 19	-28 ± 12	
Ser[17]	-143 ± 43	34 ± 8		Ser[17]	-65 ± 21	-28 ± 15	
Nle[18]	-124 ± 45	-177 ± 50		Nle[18]	-80 ± 22	-25 ± 11	
Glu[19]	-100 ± 104	-58 ± 17		Glu[19]	-90 ± 18	-3 ± 16	
Arg[20]	-66 ± 14	-24 ± 6		Arg[20]	-101 ± 4	-7 ± 2	
Val[21]	-87 ± 6	-39 ± 2		Val[21]	-102 ± 10	-52 ± 7	
Glu[22]	-55 ± 2	-23 ± 5		Glu[22]	-61 ± 6	-30 ± 13	
Nal[23]	-76 ± 4	-26 ± 1		Nal[23]	-66 ± 12	-38 ± 9	
Leu[24]	-84 ± 2	-47 ± 1		Leu[24]	-82 ± 9	-47 ± 4	
Arg[25]	-54 ± 2	-26 ± 45		Arg[25]	-61 ± 5	-34 ± 3	
Lys[26]	-87 ± 7	-14 ± 3		Lys[26]	-70 ± 7	-27 ± 6	
Lys[27]	-84 ± 4	-30 ± 4		Lys[27]	-94 ± 7	-23 ± 4	
Leu[28]	-87 ± 4	-41 ± 3		Leu[28]	-87 ± 5	-31 ± 2	
Gln[29]	-64 ± 3	-26 ± 7		Gln[29]	-78 ± 7	-28 ± 4	
Asp[30]	-84 ± 3	-30 ± 8		Asp[30]	-85 ± 5	-26 ± 4	
Val[31]	-77 ± 4	-15 ± 3		Val[31]	-84 ± 4	-16 ± 3	
His[32]	-84 ± 8	-15 ± 1		His[32]	-91 ± 9	-20 ± 7	
Asn[33]	-103 ± 8	3 ± 1		Asn[33]	-102 ± 12	-3 ± 7	
Tyr[34]	-86 ± 6			Tyr[34]	-110 ± 28		

point-mutated hybrid and converted it into a pure antagonist, while the opposite effect was observed for the PTH/PTHrP point-mutated hybrid (conversion from a pure antagonist to a weak, partial agonist).

The structural effects of insertion of a single β-Ala residue in a helical sequence have not been systematically investigated. Quite recently, Benedetti and co-workers (*42*) studied linear tri-, tetra- and pentapeptides containing alternating L-Leu and β-homo L-Leu sequences. In solvent systems such as CD_3CN or TFE/H_2O 80:20 (v/v) these compounds were found unordered, as expected for such short linear peptides. However, these authors concluded that in the solid state the overall conformation of the unprotected tripeptide H-Leu−Leu−Leu-OH is not affected by the insertion of β-homo L-Leu in position 2. Well-defined and stable helical conformations different from the α-helix were observed in oligo β-peptides containing stereogenic centers or constraints in the peptide backbone (*43*, *44*).

Interestingly, our NMR and structural calculations results showed that the insertion of a single β-amino acid residue around position 12 does not reduce the ordered structure in this segment of the sequence. In analogues **III**, **IV**, and **VI**, the β-amino acid residue is comprised in a helical segment which includes Gly[12]. Thus, in our case, the presence of a single β-amino acid residue is compatible with the helical structure around position 12.

In conclusion, in the present paper we have shown that the main effect of the substitutions with β-amino acids around position 12 of PTH-(1−34) is on the structure of the N-terminal segment. The results presented here underline the importance of the stability of the N-terminal helix as a structural determinant for bioactivity and also the relevance of the Leu[11] side-chain, presumably involved in an hydrophobic interaction with a complementary site of the PTH1 receptor.

In none of the NOESY spectra of the analogues studied in the present work were long-range connectivities detected between residues comprised within the two helical segments. Thus, consistent with the results of our previous work (*8*, *9*, *19*−*21*), these findings do not provide any evidence for the proposed U-shaped tertiary structure as the bioactive conformation (*13*), at least in the membrane-mimetic solvent medium used in our work.

Taken together, the results presented in this paper are consistent with our working hypothesis of the importance of hinges or flexible regions connecting the N- and C-terminal helices. The nonhelical flexible segment connecting the two helical segments is present and shifted to the sequence following position 13.

In two recent papers, it was proposed that PTH-(1−34) analogues bind to the receptor in an extended helical conformation (*45*, *46*). Condon et al. (*45*) carried out a CD study on several potent agonists of hPTH-(1−31) and hPTH-(1−34), constrained by Lys(*i*)-to-Asp(*i*+4) side-chain-to-side-chain lactam bridges. They observed that the lactam constraints enhance, as expected, the stability of the α-helical

Table 5: Average Values of Torsion Angles ϕ, ψ, μ, and the Relative Standard Deviations Resulting from the Lowest 20 Energy Structures Calculated for Analogues **V** and **VI**

	analogue **V**				analogue **VI**		
residue	ϕ	ψ	μ	residue	ϕ	ψ	μ
Ala[1]		88 ± 70		Ala[1]		95 ± 78	
Val[2]	−39 ± 23	−35 ± 16		Val[2]	−104 ± 29	168 ± 77	
Ser[3]	−75 ± 44	−11 ± 56		Ser[3]	−170 ± 74	76 ± 76	
Glu[4]	−51 ± 48	13 ± 5		Glu[4]	37 ± 62	−42 ± 14	
Ile[5]	−108 ± 10	−38 ± 2		Ile[5]	−86 ± 11	−25 ± 8	
Gln[6]	−76 ± 3	−29 ± 9		Gln[6]	−80 ± 10	−23 ± 5	
Phe[7]	−75 ± 9	−37 ± 1		Phe[7]	−86 ± 3	−37 ± 3	
Nle[8]	−84 ± 3	−14 ± 2		Nle[8]	−73 ± 4	−31 ± 6	
His[9]	−97 ± 4	−41 ± 10		His[9]	−65 ± 4	−24 ± 4	
Asn[10]	−55 ± 4	−30 ± 5		Asn[10]	−91 ± 9	−44 ± 7	
Leu[11]	−98 ± 3	−12 ± 7		Leu[11]	−60 ± 11	−20 ± 7	
β-Ala[12]	−137 ± 8	−103 ± 5	81 ± 2	Gly[12]	−92 ± 6	−32 ± 11	
Lys[13]	−62 ± 7	−28 ± 2		β-Ala[13]	−121 ± 6	−110 ± 12	90 ± 8
His[14]	−63 ± 13	−17 ± 15		His[14]	−57 ± 6	−14 ± 5	
Leu[15]	−70 ± 31	−10 ± 31		Leu[15]	−98 ± 24	−31 ± 16	
Ser[16]	−96 ± 45	−18 ± 21		Ser[16]	−106 ± 15	37 ± 6	
Ser[17]	−108 ± 24	−13 ± 10		Ser[17]	−62 ± 14	−72 ± 70	
Nle[18]	−72 ± 15	−12 ± 6		Nle[18]	−25 ± 45	−29 ± 5	
Glu[19]	−68 ± 31	−56 ± 11		Glu[19]	−56 ± 13	−32 ± 19	
Arg[20]	−52 ± 12	−35 ± 3		Arg[20]	−75 ± 19	−18 ± 17	
Val[21]	−76 ± 7	−34 ± 2		Val[21]	−69 ± 15	−45 ± 10	
Glu[22]	−54 ± 1	−25 ± 0		Glu[22]	−65 ± 7	−19 ± 9	
Nal[23]	−77 ± 1	−37 ± 2		Nal[23]	−82 ± 7	−42 ± 1	
Leu[24]	−64 ± 2	−35 ± 1		Leu[24]	−72 ± 7	−54 ± 5	
Arg[25]	−66 ± 2	−41 ± 1		Arg[25]	−50 ± 5	−24 ± 3	
Lys[26]	−71 ± 2	−27 ± 1		Lys[26]	−58 ± 9	−33 ± 4	
Lys[27]	−77 ± 6	−37 ± 4		Lys[27]	−96 ± 14	−20 ± 21	
Leu[28]	−76 ± 5	−34 ± 4		Leu[28]	−74 ± 36	−30 ± 13	
Gln[29]	−67 ± 8	−23 ± 7		Gln[29]	−96 ± 36	−3 ± 28	
Asp[30]	−84 ± 5	−14 ± 2		Asp[30]	−79 ± 16	−20 ± 17	
Val[31]	−110 ± 1	−12 ± 1		Val[31]	−84 ± 7	−13 ± 7	
His[32]	−89 ± 4	−20 ± 4		His[32]	−80 ± 33	−8 ± 14	
Asn[33]	−95 ± 7	2 ± 1		Asn[33]	−104 ± 42	6 ± 3	
Tyr[34]	−94 ± 16			Tyr[34]	−104 ± 14		

conformation in aqueous solution containing 20% acetonitrile. The most constrained analogue, tricyclo-[Lys[13]−Asp[17], Lys[18]−Asp[22], Lys[26]−Asp[30]]hPTH-(1−31) is completely in the α-helical conformation in this medium. Addition of 40% TFE to this solvent mixture causes complete folding of all analogues into the α-helical conformation. Surprisingly, in this solvent mixture, these authors report for the tricyclo-constrained analogue, a molar ellipticity value $[\Theta]_R^{222}$ of −44,500, while the reference value reported in the literature for completely helical peptide sequences is of −34 000 ellipticity units (*31*). In our opinion, the CD data alone are insufficient to claim that these PTH analogues exist in an extended helical, receptor-binding conformation. In our previous studies on PTH-(1−34) and PTHrP-(1−34) analogues in different solvent systems (*19*−*21*), the helix content found in TFE was always much higher than in the DPC micellar system. In TFE, 75−80% helix content was observed either in active or inactive analogues. However, to reveal the possible presence of hinges or flexible points at specific locations of the highly constrained *i*-to-*i*+4 lactam containing analogues, a detailed NMR analysis was needed.

On the basis of recent literature, it is possible that the two N- and C-terminal helices of the ligand in the receptor-bound state have roughly the same orientation. Mierke et al. (*47*, *48*), on the basis of structural studies by NMR and MD calculations on peptides derived from the first extracellular loop and from the N-terminal extracellular domain in proximity to the first transmembrane domain of the receptor, recently proposed a model of the bioactive conformation. The structure of the PTH1-rc-(241−284), derived from the first extracellular loop, comprises three α-helices located in the sequences 241−244, 256−264, and 275−284. From nitroxide radical-induced relaxation studies, the authors found that the second helix lays on the surface of the membrane-mimetic micelle. Taking into account these structural features, the authors (*47*) also identified the intermolecular interactions consistent with the contact point between Leu[261] (receptor) and Lys[27] (ligand) found by Greenberg et al. (*49*). In the proposed model, the C-terminal helix of PTH-(1−34) and the 256−264 helix of the receptor are in close proximity and oriented in an antiparallel fashion. In this partial ligand−receptor model, the ligand adopts a conformation in which the two N- and C-terminal helices are roughly in the same orientation, although not precisely aligned. Again, these findings do not support a U-shaped structure as the bioactive conformation of PTH-(1−34) and PTHrP-(1−34).

Finally, Jin et al. (*46*) recently reported the crystal structure of hPTH-(1−34) at 0.9 Å resolution. They found that the hormone fragment crystallizes as a long helical dimer. The overall structure of hPTH-(1−34) is a slightly bent helix, with the bend located between residues 12 and 21. Gly[12] is in a strict helical conformation in the crystal structure. From their findings and from the fact that replacement of Gly[12] with the helix promoters Ala and Aib is biologically well tolerated, whereas substitution with the helix breakers Pro and Sar is not (*50*), Jin et al. concluded that the helical conformation around Gly[12] is essential for full biological

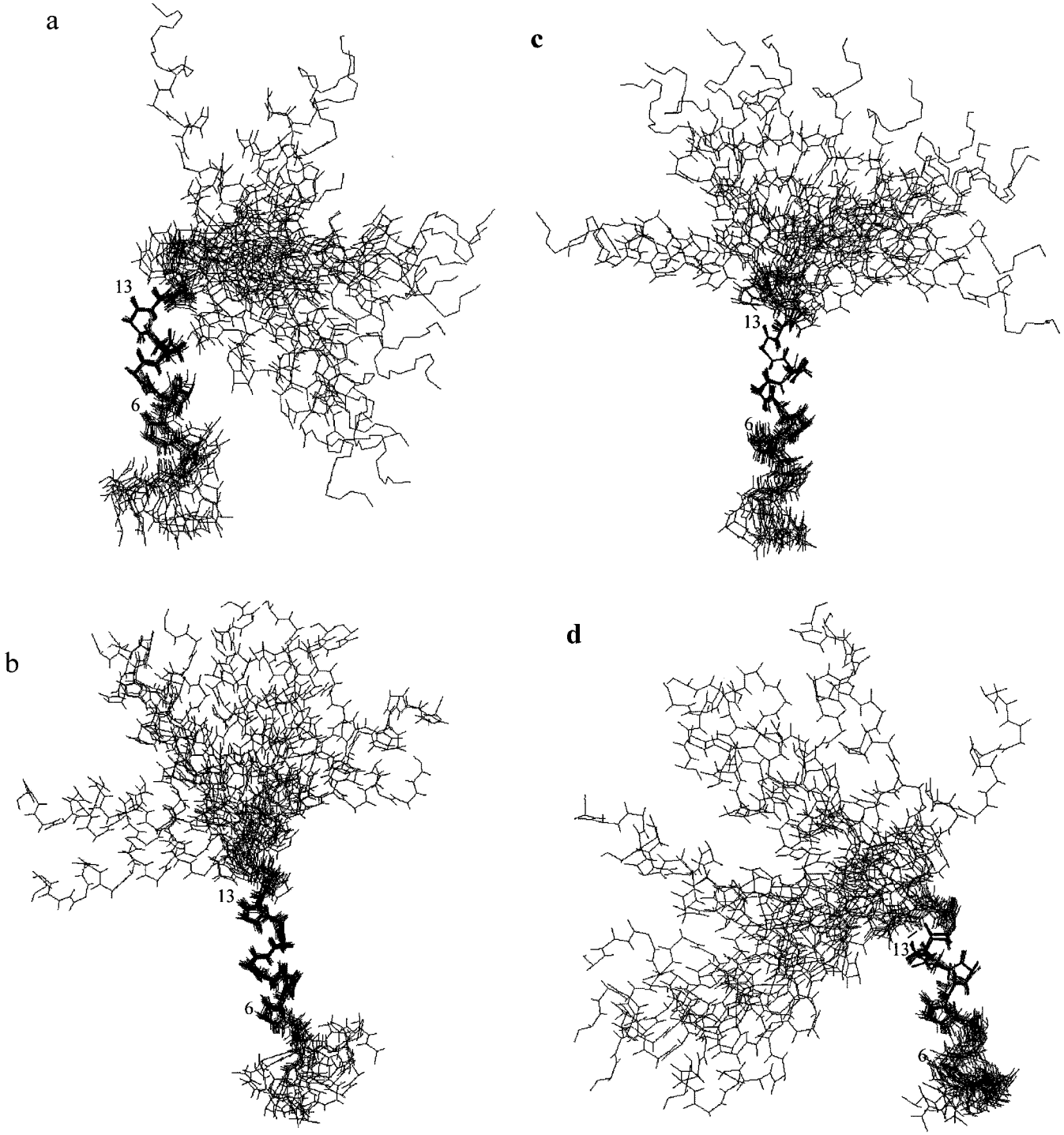

FIGURE 10: Superimposition of the ensemble of the 20 lowest energy calculated structures of analogue **III** (a), **IV (**b), **V** (c), and **VI** (d). Heavy backbone atoms of the sequence 10−14 comprising the β-amino acid residue were used in the superimposition. The carbonyl groups of residues 6 and 13 are indicated in each ensemble.

activity. On the basis of the results presented here and in previous work, the hypothesis that the crystal structure might represents the bioactive conformation of PTH-(1−34) when interacting with its cognate membrane receptor is, in our opinion, questionable. The environment experienced by the peptide chain in the crystal is rather different from a membrane or membrane-mimetic environment and, in the absence of a stable tertiary structure, packing interactions such as those leading to a dimeric form might have a predominant effect on the formation of the secondary structure.

To further assess the role of local structure around positions 12 and 19 of PTH-(1−34), we have designed new analogues containing either Aib residues around position 12 or β-amino acid residues around position 19. The results of biological evaluation and conformational analysis of these analogues will be reported in the future.

ACKNOWLEDGMENT

We are grateful to Prof. D. F. Mierke, Department of Pharmacology, Brown University, Providence, USA, for the discussions and critical reading of the manuscript. Thanks

are due to Drs. O. Perini, D. Moscon, and S. Ferguson, Department of Organic Chemistry, University of Padova, for preliminary CD and NMR measurements.

SUPPORTING INFORMATION AVAILABLE

CD spectra of analogs **I**−**V**; TOCSY and NOESY spectra of analogs **I** and **III**; and tables of proton chemical shifts of analogs **I**−**VI**. This material is available free of charge via the Internet at http://pubs.acs.org.

REFERENCES

1. Chorev, M., and Rosenblatt, M. (1994) in *Parathyroids* (Bilezikian, J. P., Levine, M. A., and Marcus, R., Eds.) 139−156, Raven Press, New York.
2. Martin, T. J., Moseley, J. M., and Gillespie, M. T. (1991) *Crit. Rev. Biochem. Mol. Biol. 26*, 277−395.
3. Gronwald, W., Schomburg, D., Tegge, W., and Wray, V. (1997) *Biol. Chem. 378*, 1501−1508, and references therein.
4. Klaus, W., Dieckmann, T., Wray, V., and Schomburg, D. (1991) *Biochemistry 30*, 6936−6942.
5. Neugebauer, W., Surewicz, W. K., Gordon, H. L., Somorjai, R. L., Sung, W., and Willick, G. E. (1992) *Biochemistry 31*, 2056−2063.
6. Strikland, L. A., Bozzato, R. P., and Kronis, K. A. (1993) *Biochemistry 32*, 6050−6057.
7. Wray, V., Federau, T., Gronwald, W., Mayer, H., Schomburg, D., Tegge, W., and Wingender, E. (1994) *Biochemistry 33*, 1684−1693.
8. Maretto, S., Mammi, S., Bissacco, E., Peggion, E., Bisello, A., Rosenblatt, M., Chorev, M., and Mierke, D. F. (1997) *Biochemistry 36*, 3300−3307.
9. Mierke, D. F., Maretto, S., Schievano, E., De Luca, D., Bisello, A., Rosenblatt, M., Peggion, E., and Chorev, M. (1997) *Biochemistry 36*, 10372−10383.
10. Barden, J. A., and Cuthbertson, R. M. (1993), *Eur. J. Biochem. 215*, 315−321.
11. Ray, F, R., Barden, J. A., and Kemp, B. E. (1993) *Eur. J. Biochem. 211*, 205−211.
12. Pellegrini M., Royo, M., Rosenblatt, M., Chorev, M., and Mierke, D. F. (1998) *J. Biol. Chem. 273*, 10420−10427.
13. Cohen, F. E., Strewler, G. J., Bradley, M. S., Carlquist, M., Nilsson, M., Ericson, M., Ciardelli, T. L., and Nissenson, R. A. (1991) *J. Biol. Chem. 266*, 1997−2004.
14. Marx, U. C., Austermann, S., Bayer, P., Adermann, K., Ejchart, A., Sticht, H., Walter, S., Schmid, F. X., Jaenicke, R., Forssmann, W. G., and Rösch, P. (1995) *J. Biol. Chem. 270*, 15194−15202.
15. Marx, U. C., Adermann, K., Bayer, P., Meyer, M., Forssmann, W. G., and Rösch, P. (1998) *J. Biol. Chem. 273*, 4308−4316.
16. Weidler, M., Marx, U. C., Seidel, G., Schäfer, W., Hoffman, E., Esswein, A., and Rösch, P. (1999) *FEBS Lett. 444*, 239−244.
17. Marx, U. C., Adermann, K., Bayer, P., Forssmann, W. G., and Rösch, P. (2000) *Biochem. Biophys. Research Commun. 267*, 213−220.
18. Chen, Z., Xu, P., Barbier, J. R., Willick, G., and Ni, F. (2000) *Biochemistry 39*, 12766−12777.
19. Peggion, E., Mammi, S., Schievano, E., Behar, V., Rosenblatt, M., and Chorev, M. (1999) *Biopolymers 50*, 525−535.
20. Schievano, E., Mammi, S., Silvestri, L., Behar, V., Rosenblatt, M., Chorev, M., and Peggion, E. (2000) *Biopolymers 54*, 429−447.
21. Maretto, S., Schievano, E., Mammi, S., Bisello, A., Nakamoto, C., Rosenblatt, M., Chorev, M., and Peggion, E. (1998) *J. Pept. Res. 52*, 241−248.
22. Merrifield, R. B. (1963) *J. Am. Chem. Soc. 85*, 2149−2154.
23. Bisello, A., Adams, A. E., Mierke, D. F., Pellegrini, M., Rosenblatt, M., Suva, L. J., and Chorev, M. (1998) *J. Biol. Chem. 273*, 22498−22505.
24. Zhou, A. T., Bessalle, R., Bisello, A., Nakamoto, C., Rosenblatt, M., Suva, L. J., and Chorev, M. (1997) *Proc. Natl. Acad. Sci. U.S.A. 94*, 3644−3649.
25. Nakamoto, C., Behar, V., Chin, K. R., Adams, A. E., Suva, L. J., Rosenblatt, M., and Chorev, M. (1995) *Biochemistry 34*, 10546−10552.
26. Goldman, M. E., Chorev, M., Reagan, J. E., Nutt, R. F., Levy, J. J., and Rosenblatt, M. (1988) *Endocrinology 123*, 1468−1475.
27. Rodan, S. B., Wesolowski, G., Ianacone, J., Thiede, M. A., and Rodan, G. A. (1989) *J. Endocrinol. 122*, 219−227.
28. Roubini, E., Duong, L. T., Gibbons, S. W., Leu, C. T., Caulfield, M. P., Chorev, M., and Rosenblatt, M. (1992) *Biochemistry 31*, 4026−4033.
29. Pines, M., Adams, A. E., Steuckle, S., Bessalle, R., Rashti-Behar, V., Chorev, M., Rosenblatt, M., and Suva, L. J. (1994) *Endocrinology 135*, 1713−1716.
30. Solomon, Y., Londos, C., and Rodbell, M. A. (1974) *Anal. Biochem. 58*, 541−548.
31. Greenfield, N., and Fasman, G. D. (1969) *Biochemistry 8*, 4108−4116.
32. Sklenar, V., Piotto, M., Leppik, R., and Saudek, V. (1993) *J. Magn. Reson. Series A 102*, 241−245.
33. Rance, M., Sørensen, O. W., Bodenhausen, G., Wagner, G., Ernst, R. R., and Wüthrich, K. (1983) *Biochem. Biophys. Res. Commun. 117*, 479−485.
34. Bax, A., and Davis, D. G. (1985) *J. Magn. Reson. 65*, 355−360.
35. Griesinger, C., Otting, G., Wüthrich, K., and Ernst, R. R. (1988) *J. Am. Chem. Soc. 110*, 7870−7872.
36. Macura, S., Huang, Y., Suter, D., and Ernst, R. R. (1980) *J. Magn. Reson. 43*, 259−281.
37. Cavanagh J., Waltho J. P., and Keeler, J. (1987) *J. Magn. Reson. 74*, 386−393.
38. Neidig, K. P. (1996) *Aurelia Software Manual (version 2.1)*, Bruker Analytic GmbH, Karlsruhe, Germany.
39. Brünger, A. T. (1992) *X-PLOR Manual (version 3.0)*, Yale University, CT.
40. Pastore, A., and Saudek, V. (1990) *J. Magn. Reson. 90*, 165−176.
41. Nutt, R. F., Caufield, M. P., Levy, J. J., Gibbons, S. W., Rosenblatt, M., and McKee, R. L. (1990) *Endocrinology 127*, 491−493.
42. Rossi, F., Bucci, E., Isernia, C., Iacovino, R., Romanelli, A., Di Lello, P., Grimaldi, M., Montesarchio, D., De Napoli, L., Piccialli, G., and Benedetti, E. (2000) *Biopolymers 53*, 140−149.
43. Seebach, D., and Matthews, J. L. (1997) *Chem. Commun.* 2015−2022, and references therein.
44. Appella, D. H., Christianson, L. A., Karle, I. L., Powell, D. R., and Gellman, S. H. (1996) *J. Am. Chem. Soc. 118*, 13071−13072, and references therein.
45. Condon, S. M., Morize, I., Darnbrough, S., Burns, C. J., Miller, B., E., Uhl, J., Burke, K., Jariwala, N., Locke, K., Krolikowsky, P. L., Kumar, N. V., and Labaudinier, R. F. (2000) *J. Am. Chem. Soc. 122*, 3007−3014.
46. Jin, L., Briggs, S. L., Chandrasekhar, S., Chirgadze, Y., Clawson, D. K., Schewitz, R. W., Smiley, D. L., Tashjian, A. H., and Zhang, F. (2000) *J. Biol. Chem. 275*, 27238−27244.
47. Piserchio, A., Bisello, A., Rosenblatt, M., Chorev, M., and Mierke, D. F. (2000) *Biochemistry 39*, 8153−8160.
48. Pellegrini, M., Bisello, A., Rosenblatt, M., and Mierke, D. F. (1998) *Biochemistry 37*, 12737−12743.
49. Greenberg, Z., Bisello, A., Mierke, D. F., Rosenblatt, M., and Chorev, M. (2000) *Biochemistry 39*, 8142−8152.
50. Chorev, M., Goldman, M. E., McKee, R. L., Roubini, E., Levy, J. J., Gay, C. T., Reagan, J. E., Fisher, J. E., Caporale, L. H., Golub, E. E., Caulfield, M. P., Nutt, R. F., and Rosenblatt, M. (1990) *Biochemistry 29*, 1580−1586.

BI0200155